ARMY RESEARCH LABORATORY

Atmospheric Soundings in Near Real Time from Combined Satellite and Ground-Based Remotely Sensed Data

By James Cogan
Edward Measure
Information Science and Technology Directorate
Battlefield Environment Division

and
Daniel Wolfe
National Oceanic and Atmospheric Administration

ARL-TR-1481 October 1997

The findings in this report are not to be construed as an official Department of the Army position unless so designated by other authorized documents.

Citation of manufacturer's or trade names does not constitute an official endorsement or approval of the use thereof.

REPORT DOCUMENTATION PAGE	Form Approved OMB No. 0704-0188

1. AGENCY USE ONLY (Leave Blank)	2. REPORT DATE	3. REPORT TYPE AND DATES COVERED
	October 1997	Technical Report

4. TITLE AND SUBTITLE

Atmospheric Soundings in Near Real Time from Combined Satellite and Ground-Based Remotely Sensed Data

5. FUNDING NUMBERS

6. AUTHOR(S)

James Cogan, Edward Measure (ARL)
Daniel Wolfe (NOAA)

7. PERFORMING ORGANIZATION NAME(S) AND ADDRESS(ES)

U.S. Army Research Laboratory
Information Science and Technology Directorate
Battlefield Environment Division
ATTN: AMSRL-IS-EA
White Sands Missile Range, NM 88002-5501

8. PERFORMING ORGANIZATION REPORT NUMBER

ARL-TR-1481

9. SPONSORING/MONITORING AGENCY NAME(S) AND ADDRESS(ES)

U.S. Army Research Laboratory
2800 Powder Mill Road
Adelphi, MD 20783-1145

10. SPONSORING/MONITORING AGENCY REPORT NUMBER

ARL-TR-1481

11. SUPPLEMENTARY NOTES

12a. DISTRIBUTION/AVAILABILITY STATEMENT

Approved for public release; distribution is unlimited.

12b. DISTRIBUTION CODE

A

13. ABSTRACT (Maximum 200 words)

This report describes the theory, design, and performance of a mobile system for remotely measuring atmospheric wind, temperature, and moisture profiles for determination of artillery meteorological corrections. The principal components, their principles of operation, and the method for combining their resulting measurements are described. The results of comparisons of measurements made by the prototype system with radiosonde and pibal measurements are presented.

14. SUBJECT TERMS

atmospheric profiler, temperature, winds, radar, radiometry, satellite, meteorology

15. NUMBER OF PAGES

57

16. PRICE CODE

17. SECURITY CLASSIFICATION OF THIS REPORT	18. SECURITY CLASSIFICATION OF THIS PAGE	19. SECURITY CLASSIFICATION OF ABSTRACT	20. LIMITATION OF ABSTRACT
UNCLASSIFIED	UNCLASSIFIED	UNCLASSIFIED	SAR

Preface

First-round, fire-for-effect artillery fire requires accurate knowledge of the meteorological parameters affecting the trajectory; namely, vertical profiles of temperature, wind, and density. Traditionally, these profiles have been measured using the balloon-borne radiosonde. The radiosonde is accurate and has been extremely well tested over the last 60 years, but it also has serious disadvantages due to its lack of timeliness and long logistical "tail" (because it requires a helium or hydrogen supply for its balloons).

The Mobile Profiling System (MPS) described herein can overcome these temporal and logistical problems by automated, near real-time remote sensing methods.

Acknowledgements

The authors acknowledge Florence Patten and Judy Kilmon of the Wallops Flight Facility (WFF), NASA, who supplied the pibal data at Wallops Island; and John Cruncleton and Richard Okrasinski who provided key assistance in the computer drawing of figures 3 through 12.

Contents

Figures

Tables

Executive Summary

A mobile atmospheric profiling system has been developed by the Battlefield Environment Division (BED) of the U.S. Army Research Laboratory (ARL) and the Environmental Technology Laboratory (ETL) of the Environmental Research Laboratories, National Oceanic and Atmospheric Administration (NOAA). This system, which is capable of probing the atmosphere from the surface to altitudes over 30 km, combines ground-based instruments, including a five-beam, 924 MHz radar wind profiler; a Radio Acoustic Sounding System (RASS); and two passive microwave sounders (measuring virtual temperature and moisture parameters, respectively) with a receiver and processor for meteorological satellite images and soundings.

This report describes the method for merging data from satellite and ground-based remote sensing systems and presents results of early tests of the Mobile Profiler System (MPS), including information on accuracies achieved in its measurements. Examples of some of the many data formats produced by the MPS are also shown.

Software in the MPS produces profiles from the surface to the highest satellite sounding level by combining profiles generated from the suite of ground-based sensors with those from a meteorological satellite. The algorithms generate soundings of temperature, humidity, wind velocity, and other meteorological variables.

The MPS combines the capabilities of several types of sensing systems to provide atmospheric soundings with a rapid refresh rate that greatly reduces errors caused by time staleness. The ability of the ground-based instruments in the MPS to generate a picture of very short patterns and changes in atmospheric variables in the lower troposphere can lead to a better understanding of the atmosphere and better modeling at smaller scales.

Future plans for the MPS include development of a much more compact version with improved mobility and capability.

The MPS has operated successfully in different climates, including operations during the Los Angeles Free Radical Experiment (LAFRE) in Claremont, CA, and tests at White Sands Missile Range (WSMR), NM, Erie, CO, Ft. Sill, OK, and Wallops Island, VA.

1. Introduction

1.1 Background

Ground-based systems currently in use for operational measurement of atmospheric profiles rely heavily on balloon-borne rawinsondes. The time between balloon launches may be as little as 1 to 4 h during field experiments, but in normal operations launches occur every 12 hours. The National Oceanic and Atmospheric Administration's (NOAA) National Profiler Network (NPN), consisting of 404 MHz radars at fixed sites mostly in the central United States, can provide wind profiles every hour. [1, 2, 3, 4] Some sites are also equipped with Radio Acoustic Sounding Systems (RASS), providing profiles of virtual temperature (T_v). Meteorological satellite sounders using either infrared or microwave wavelengths provide a means of obtaining atmospheric soundings on a routine basis for regions where surface and upper-air stations are absent. However, for mesoscale areas over land, satellite sounder data may have horizontal and vertical resolutions that are too coarse for certain applications, especially for the lower troposphere. Orlanski defines various mesoscale size ranges. [5]

In the lowest 1 or 2 km of the troposphere over land, satellite temperature (T) soundings without ancillary data generally have errors of as much as 5 to 8 °K. [6, 7, 8] For derived variables such as wind velocity the margin for error may be even greater. [9] Vertical and horizontal resolutions are typically about 3 to 5 km and 30 to 200 km, respectively, depending on whether infrared or microwave sounders are used and on the amount of spatial averaging for noise reduction. [10, 11, 12]

1.2 The Mobile Profiler System

The Mobile Profiling System (MPS), currently being developed by the U. S. Army Research Laboratory (ARL) and NOAA's Environmental Technology Laboratory (ETL), can provide soundings in the troposphere as often as once every 3 min. [13] The radar wind profiler operating at 924 MHz can provide wind profiles with a vertical resolution of 100 m up to an average height of 3 to 5 km, depending on atmospheric conditions. Under certain atmospheric conditions (i.e., moist and turbulent) heights over 6 km are possible. The RASS can produce soundings of T_v up to 0.8 to 1.6 km at a vertical resolution of about 100 m (again depending on atmospheric conditions). A microwave radiometer operating in the oxygen band from 50 to 60 GHz is able to produce useful T_v

profiles to altitudes of 3 to 5 km. A second radiometer produces estimates of total water content (vapor and liquid). A new radiometer currently under evaluation will replace both older radiometers in a package smaller than either.

The MPS receives direct read-out data from the NOAA's series of polar-orbiting satellites. The satellite receiver and processor system is being upgraded to a smaller but more capable version that will be able to obtain direct read-out data from Defense Meteorological Satellite Program (DMSP) satellites.

The MPS has certain elements in common with fixed-site systems described by Parsons et al. and Stokes and Schwartz, but it also has a number of additional features. [14, 15] These additions include software for processing and quality-controlling data from the ground-based sensors, and for combining satellite soundings with ground-based profiles in near real time. Wolfe et al. provide details about the MPS as it was configured and operated during the Los Angeles Free Radical Experiment (LAFRE) in Claremont, CA, and present examples of the various data processing and output available. [13] Cogan and Izaguirre present additional samples of output and give preliminary quantitative results. [16] Figure 1, from Wolfe et al., shows the primary sensors in the MPS as configured during the LAFRE. [13] Table 1 presents certain MPS instrument characteristics and compares the LAFRE configuration with the MPS with recent and ongoing changes.

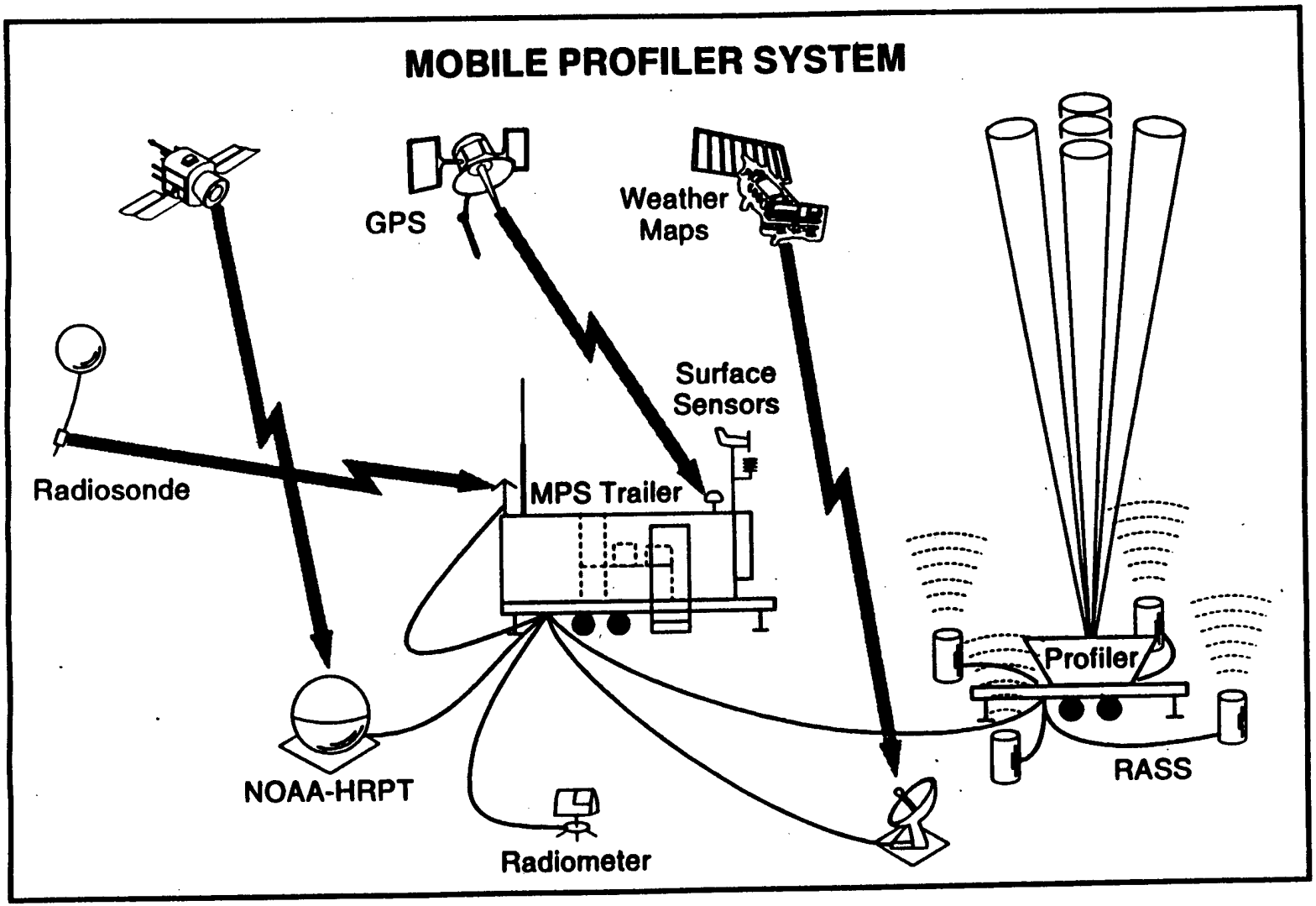

Figure 1. Layout of primary components of the MPS, from Wolfe et al. (1995).

Table 1. MPS sensors and characteristics. Initial configuration compared with that with recent and ongoing upgrades. New version has smaller, more robust shelter for processors and some instruments

System	Initial MPS as during LAFRE	MPS with new/ongoing upgrades
Radar wind profiler	924 MHz, phased array	Combined phased array wind radar (924 MHz) and RASS (~2000 Hz), 120 transducers in RASS
RASS	~2000 Hz, 4 external sources	
MW Radiometer	T: 50-60 GHz (O_2); PW, LW: 22.7, 31.4 GHz, 2 radiometers (T, PW/LW)	One radiometer opertating in same frequency bands for some variables, smaller than either of older radiometers
Satellite receiver and processor	HRPT from NOAA satellites (soundings and imagery)	Upgraded, smaller system: HRPT from NOAA and direct read-out DMSP
Portable surface station	Standard meteorological variables, on trailer-mounted mast	No change
Weather map receiver	Receive maps and other data via GOES	Eliminated GOES link, maps and other weather data via Internet
GPS receiver	Provides site location	No change

1.3 Overview

The merging method for combining ground-based and satellite profiles described in this report is a revised version of the technique described in Cogan and Izaguirre. [17] This method may be used for T_v, pressure, wind velocity, and other meteorological variables. Even though the microwave radiometer component of the MPS uses a statistical method for retrieval of temperature profiles and moisture parameters that requires *a priori* data, the merging algorithm itself may be applied wherever the MPS is located (i.e., it is not site-specific and requires no *a priori* information). However, the user may alter certain software parameters (e.g., output layer thickness or maximum distance from the MPS site for acceptance of satellite profiles). Current statistical techniques for merging ground-based and satellite profiles of T (or T_v) reported in the literature are site-specific in that statistical coefficients are computed using a large set of *a priori* data normally gathered for a long series of rawinsonde soundings from a particular location. [18, 19, 20] In this report we discuss characteristics of instruments of the type employed in the MPS and describe the method for merging satellite and ground-based profiles into a combined sounding. We present results of field tests of both combined soundings and profiles from individual ground-based sensors. Comparisons with rawinsondes and radar-tracked pibals give an idea of how these systems compare with more traditional sounding systems.

2. Sensor Characteristics

Before evaluating the merging algorithm and accuracies of the component sensors, the accuracies and other relevant measurement parameters of similar data sources from the formal literature should be examined. Of particular interest are the satellite sounders and ground-based radar profilers, RASS, and microwave radiometers of the type used in the MPS. Table 2 summarizes selected information extracted from Moran and Strauch, Flowers et al., Okrasinski and Olsen, Weber and Wuertz, Weber et al., Reale, May et al., Le Marshall, Franklin and Lord, and Jedlovec. [21, 22, 23, 24, 3, 8, 25, 7, 9, 6] These values may be compared with similar data for common rawinsonde systems (Fisher et al.), also presented in table 2. [26]

Table 2. Capabilities of several remote sensing and rawindsonde systems. The values shown represent averages for most current systems in each group.

System	Capabilities				
	Variable	Accuracy	Temporal resolution	Vertical resolution	Vertical range
Radar Profiler 915/924 MHz	wind speed	± 1.5 to 3 ms^{-1}	3 to 6 min (Consensus methods may need up to 30 min)	100 m	100 to 5000 m
	wind direction	± 10 to 15°			
RASS	virtual temperature	± 1 to 2° K			100-1600 m
Microwave Radiometer	temp. or virtual temp.	± 1 to 3° K	3 min	variable	up to 10 km
Satellite Sounder (TOVS, SSM/T-1)	temperature	± 2 to 2.5° K	5 h (2 Sat) 4 h (3 Sat) (1 to 2 h near poles)	3 to 5 km	2 to 40 km
	wind speed	± 4 to 14 ms^{-1}			
	wind direction	± 10 to 30°			
Rawindsonde	temperature	± 0.5 to 1° K	1 to 3 h depending on maximum height	point value 60 to 600 m layers	Surface to 30 km
	wind speed	± 0.5 to 2 ms^{-1}			
	wind direction	± 5 to 10°			

From table 2 we see that ground-based radar profilers and RASS have accuracies that approach those of some operational rawinsonde systems. Flowers et al. note that the RASS performance may be reduced under certain conditions (e.g., strong near-surface winds), and the extreme cases they reported are not included in the table. [22] All the systems in table 2 produce measurements of a volume or layer average, except rawinsonde values of T. A radar profiler obtains a mean wind over a volume, with a horizontal scale on the order of tens

to thousands of meters depending on altitude from the radar, beam elevation angle, and beamwidth. For a system such as 404, 449, or 50 MHz radars, the volume represented by the three (or five) beams used to measure the horizontal and vertical wind may have a horizontal diameter exceeding 10 km near 15 or 20 km altitude. The radar processing algorithms developed by ETL for the MPS (Wolfe et al.) represent an improvement over the standard consensus techniques. [13] These algorithms allow for higher data quality at faster data rates than previously possible. Errors in wind measurements caused by migratory birds (Wilczak et al.) have been addressed through a new spectral averaging method (Merritt). [27, 28] Although limited when bird densities are high, this algorithm attempts to identify interference in the spectral data prior to averaging, thereby retaining more useful wind information.

Vertical profiles of T_v can be inferred from measurements of microwave brightness temperatures. For surface-based measurements, in the 20 to 60 GHz region, the measured brightness temperatures approximately satisfy the following equation:

$$T_{bv} = \int_0^\infty T(z)\alpha_v(z)\exp\left[-\int_0^z \alpha_v(z')dz'\right]dz + T_{bv}^\infty \exp\left[-\int_0^\infty \alpha_v(z)dz\right] \qquad (1)$$

where T_{bv} is the downwelling microwave brightness temperature at frequency v; $T(z)$ is temperature at height z; $\alpha_v(z)$ is the absorption coefficient; T^∞_{bv} is the downwelling cosmic microwave background brightness temperature above the atmosphere.

Inferring atmospheric temperature structure from microwave brightness temperature measurements thus becomes the problem of solving (inverting) equation (1) to find $T(z)$. A database of past radiosonde observations has been used to calculate corresponding received radiances at our operating frequencies. Our temperature profiles are calculated with regression coefficients computed from the database radiances and corresponding radiosonde observations. The absorption coefficient $\alpha_v(z)$ in the frequency region of interest is due mainly to oxygen lines (50 to 60 GHz), the water vapor line at 22.235 GHz, and a liquid water continuum measured near 31.4 GHz. Oxygen is well mixed in the atmosphere, so a good *a priori* estimate of its contribution is possible. In our scheme, water vapor and liquid water are independently measured by radiometric channels near 22.235 and 31.4 GHz. Vertical resolution is about 30 m at heights below 1 km, increasing to more than 1 km around 10 km.

Satellite sounders measure radiances that are converted to temperatures that represent means for large volumes of atmosphere, according to the frequency-dependent weighting functions and horizontal field of view. Temporal resolutions in table 2 are average values. Generally, satellite values are valid for altitudes > 2 or 3 km above a land surface and not near the tropopause (e.g., T to + 5 to 8 °K near the surface, and + 3 to 5 °K near the tropopause). A temperature may represent the mean over a vertical extent of 3 to 5 km and over a horizontal area of tens to over 100 km diameter (assuming a circular area). Wind velocity is derived from the satellite temperature profile using geostrophic, gradient, or thermal wind equations (Franklin and Lord). [9] A rawinsonde acquires a mean-layer wind velocity along its path, over a period of perhaps 1 min or less (most rawinsondes rise at about 5 ms^{-1}). Its temperature measurements may be considered as point values. Temporal resolution of < 1 h may be achieved for rawinsondes if there is a capability for multiple transmitter frequencies. Table 2 provides an indicator of the relative "quality" of data from the listed sensors inclusive of inherent differences between them due to measurement and processing methods. However, satellite sounders are the only means of obtaining large-area or global coverage, while radar profilers with RASS and microwave radiometers have the best spatial and temporal resolution.

3. Merging Algorithms

The algorithms described in this section combine profiles from a suite of ground-based systems and satellite sounders. Radar profiler, RASS, and microwave radiometer provide data below the lowest satellite level. Currently, RASS values of T_v are used up to the highest RASS data level. Above that height radiometer values are used, when available, up to the maximum height of "useful" data (nominally about 3.5 km based on early test results). The combined RASS and radiometer profile is the ground-based profile of T_v. Where ground-based and satellite profiles overlap, the satellite data are weighted in accordance with the spatial and temporal separation of the sounding from the ground-based profiles. The radar wind profiler, RASS, and radiometer combination will hereafter be referred to collectively as the profiler. The spatial weighting function has an elliptical form:

$$W = 1 - X^2/A^2 - Y^2/B^2 \qquad (2)$$

where W is weight, A and B are the semi-major and semi-minor axes of the assumed elliptical area represented by the satellite sounding (> the horizontal resolution of a single satellite profile), and X and Y are the distances along those axes from the profiler to the center of the satellite sounding footprint. For polar-orbiting satellites a circular area may be sufficient away from the edges of the swath, say within 500 or 600 km of the subsatellite track. Some misregistration with height can occur as nadir angle increases, especially towards the edges of the swath. The temporal weighting function has an initial period when the two sources of data have equal weight (e.g., 15 min), followed by a period of linear decrease to some time (usually 3 to 6 h) when the satellite data are ignored (temporal weight = 0). The final weight given to the satellite sounding is the product of the spatial and temporal weights times an accuracy ratio (R). This ratio relates typical accuracies (table 2) of the radar wind profiler, RASS (T_v), and radiometer (T or T_v estimate) to those of the satellite sounder. For current instruments, R decreases the weight given to the satellite data. The user may alter these parameters.

The satellite and ground-based profiles may overlap, or a gap may occur between them. When the profiles overlap, the satellite data are interpolated to profiler heights in the overlap region. The equation for combining the two sets of data for those heights has the following form:

$$Q = W(Q_p + Q_s)/2 + (1 - W)Q_p \quad (3)$$

where Q is a variable at some height, W is here the combined temporal and spatial weight times the accuracy ratio R, and subscripts $_p$ and $_s$ refer to profiler and satellite, respectively.

Where the data do not overlap, a gap exists between the highest altitude of a ground-based profile and the lowest height of the satellite data. In this case the satellite data are extrapolated down to the maximum altitude of the ground-based profile. Above the highest altitude of the profiler data for either T_v or wind velocity, the satellite value is adjusted according to a scheme described in Cogan and Izaguirre. [17] It is based on the difference between satellite (actual or extrapolated) and profiler values at the maximum profiler height for the particular variable. The adjustment or correction is reduced in magnitude through multiplication by an adjustment parameter (α) at successive heights up to a preset number of satellite levels (i.e., $D_i = \alpha[D_{i-1}]$, where D is the difference value, and $_i$ is a satellite sounding level). Normally data are adjusted for three to five satellite levels above the highest profiler level. The adjustment parameter α and the number of levels may be altered by the user. If the gap between the highest profiler level and the satellite level immediately above exceeds a preset value (e.g., 2 or 3 km) the algorithm skips the extrapolation routine and does not adjust the satellite data. Each satellite T profile is converted to T_v using retrieved dew points, if available; otherwise the program uses a rough estimate based on the surface value of humidity. Alternatively, a profile based on, say, regional climatology could be used. At the heights of satellite data used here, > 2.5 km above ground level (AGL), T_v often is within 1 °K of T. No conversion takes place if T or dewpoint is less than 233 °K, or $z > 10$ km.

Figure 2 shows plots of combined soundings of wind velocity for the period 170 to 2000 UTC, July 29, 1994, at White Sands Missile Range (WSMR), NM. Each wind profile is a 15 min average ending at the time when the profile is plotted. Wind barbs plotted near 4.8, 6.4, and 8.3 km are satellite-derived thermal winds modified according to the aforementioned method.

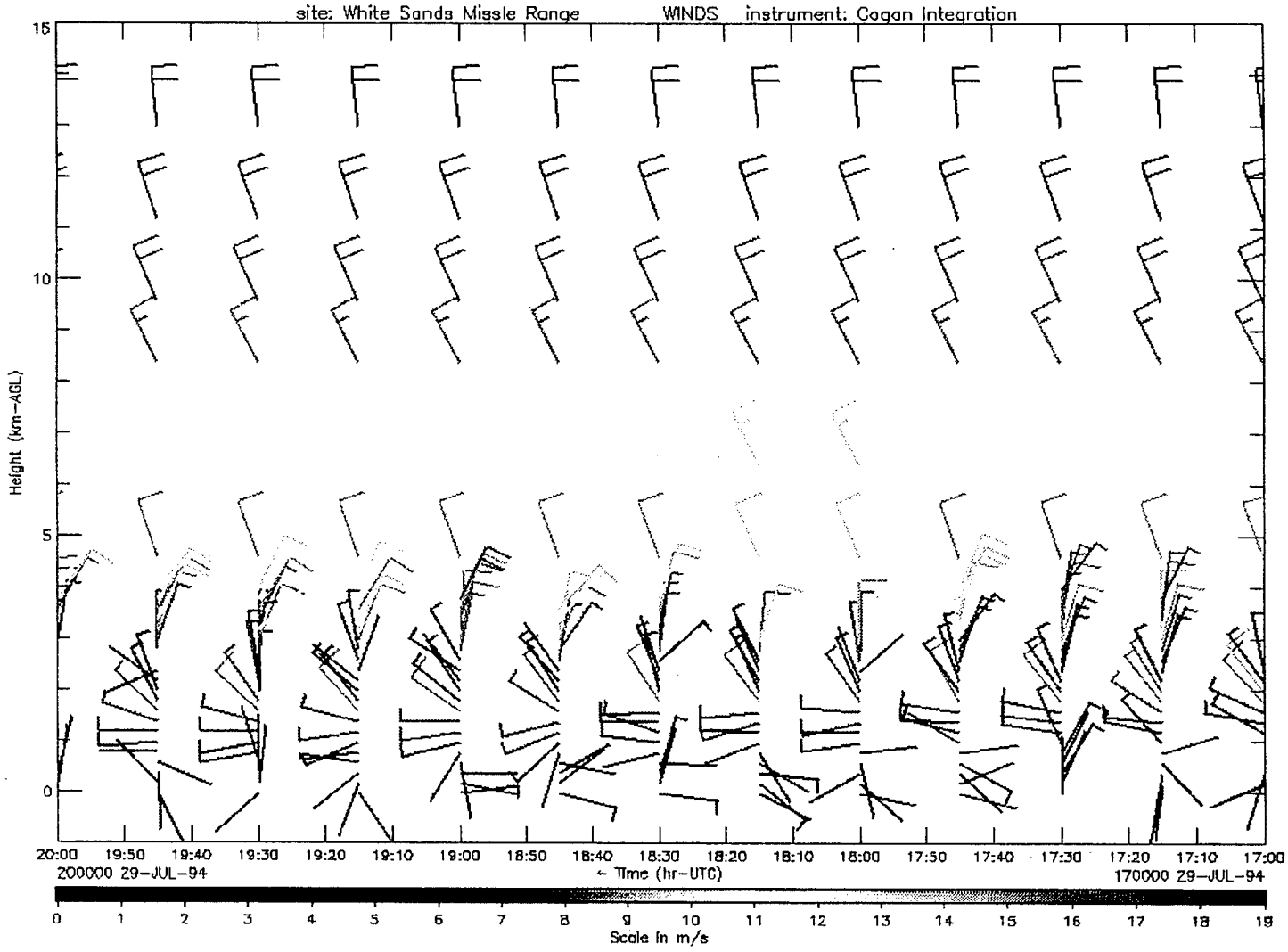

Figure 2. Time-height wind barb plot for July 29, 1994, at WSMR, NM, from Cogan. [16]

4. Results and Comparisons

4.1 Los Angeles Free Radical Experiment

Personnel from ARL and ETL participated in the Los Angeles Free Radical Experiment (LAFRE), using the MPS to obtain detailed sounding data for the primary sponsor, the California Air Resources Board. These data also served to test the system and algorithms. The MPS operated almost continuously from August 28 through September 23, 1993. During this period a MARWIN and Cross-chain Loran Atmospheric Sounding System (CLASS) were operated simultaneously from the MPS trailer. The ability to operate rawinsondes from the MPS allowed for detailed intercomparisons. Near real-time graphical and statistical comparisons were possible using software developed by ETL and ARL (Wolfe et al.; Cogan and Izagirrre). [13, 16] The microwave radiometer (temperature only) operated only during part of the LAFRE, and the merged profiles discussed here do not include microwave data.

From August 28 through September 11, 1993, the Los Angeles basin was under a strong upper ridge, and at times a closed high pressure area from the surface through 300 hPa. The marine boundary layer was consistently capped by one or more inversions. Wolfe et al., and Cogan and Izaguirre present charts that show wind velocities from the radar profiler for typical days during this early part of the LAFRE, depicting light and often variable winds. [13, 16] Combining these profiles with the nearest good satellite sounding, sometimes as much as 300 km distant, led to a "worst case" situation on several days. Atmospheric conditions, especially wind velocity, are often quite different 200 or 300 km to either side of a strong ridge.

Figures 3 through 6 show merged profiles from the LAFRE data compared with rawinsonde data for 0.1 km averaged layers. Figure 3 contains up to 36 potential comparisons during September 7 through 11, compared with a maximum of 12 during September 17 and 20 through 23 for figure 4. During the second period, comparisons were obtained on September 1 and September 20 through 23. Figures 5 and 6 show the RASS values of figures 3 and 4, respectively, in an expanded scale for heights < 2 km. For these comparisons RASS T_v values were corrected for vertical velocity in a manner similar to that employed by Moran and Strauch. [21] These results suggest that the greatest differences may occur within any layer of atmosphere, and are not uniformly distributed with height.

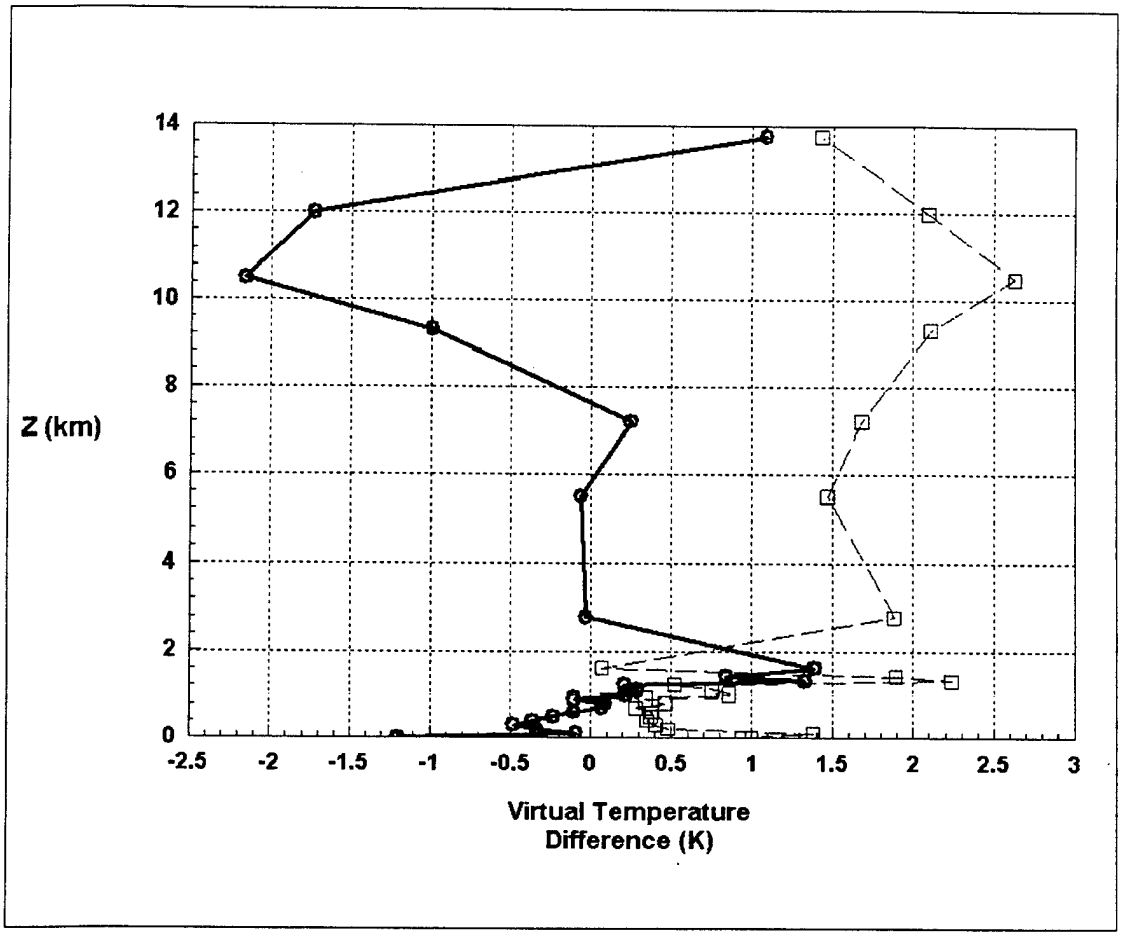

Figure 3. Mean (solid line) and standard deviation (dashed line) of T_v (°K) differences (MPS - rawindsonde) for September 7 through 11, 1993. Heights are AGL.

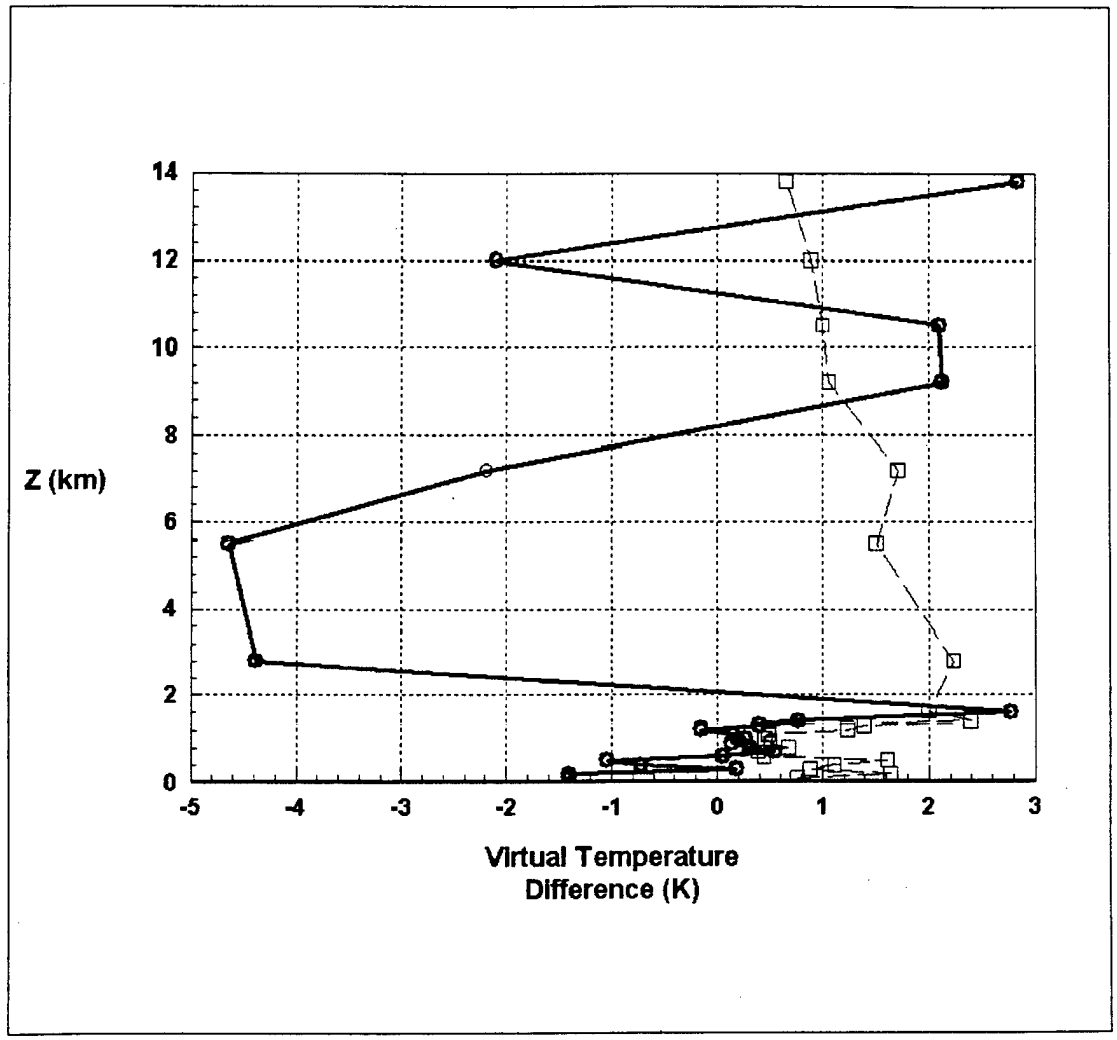

Figure 4. Same as figure 3, except for September 17 and 20 through 23, 1993. Heights are AGL.

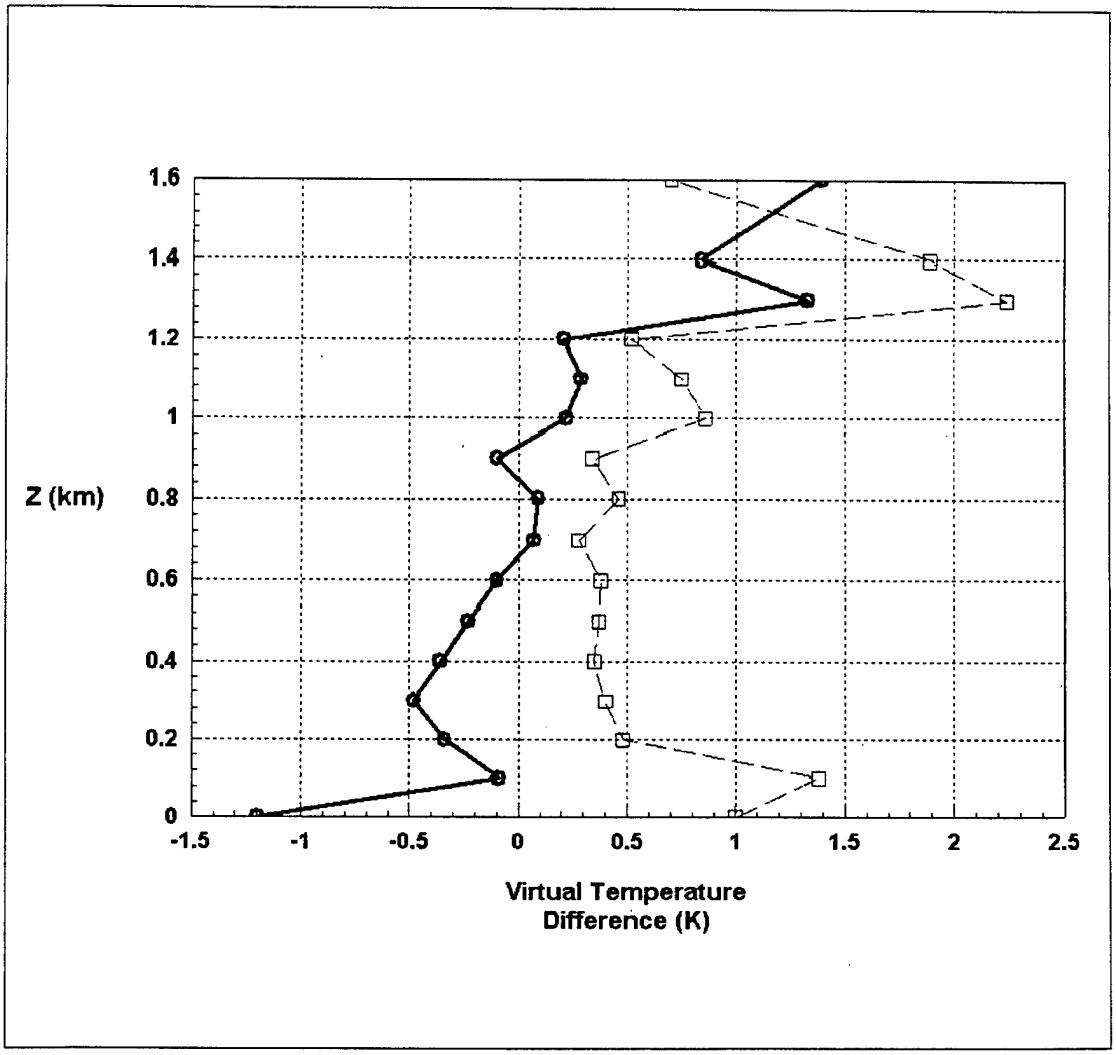

Figure 5. Same as figure 3, but for RASS only.

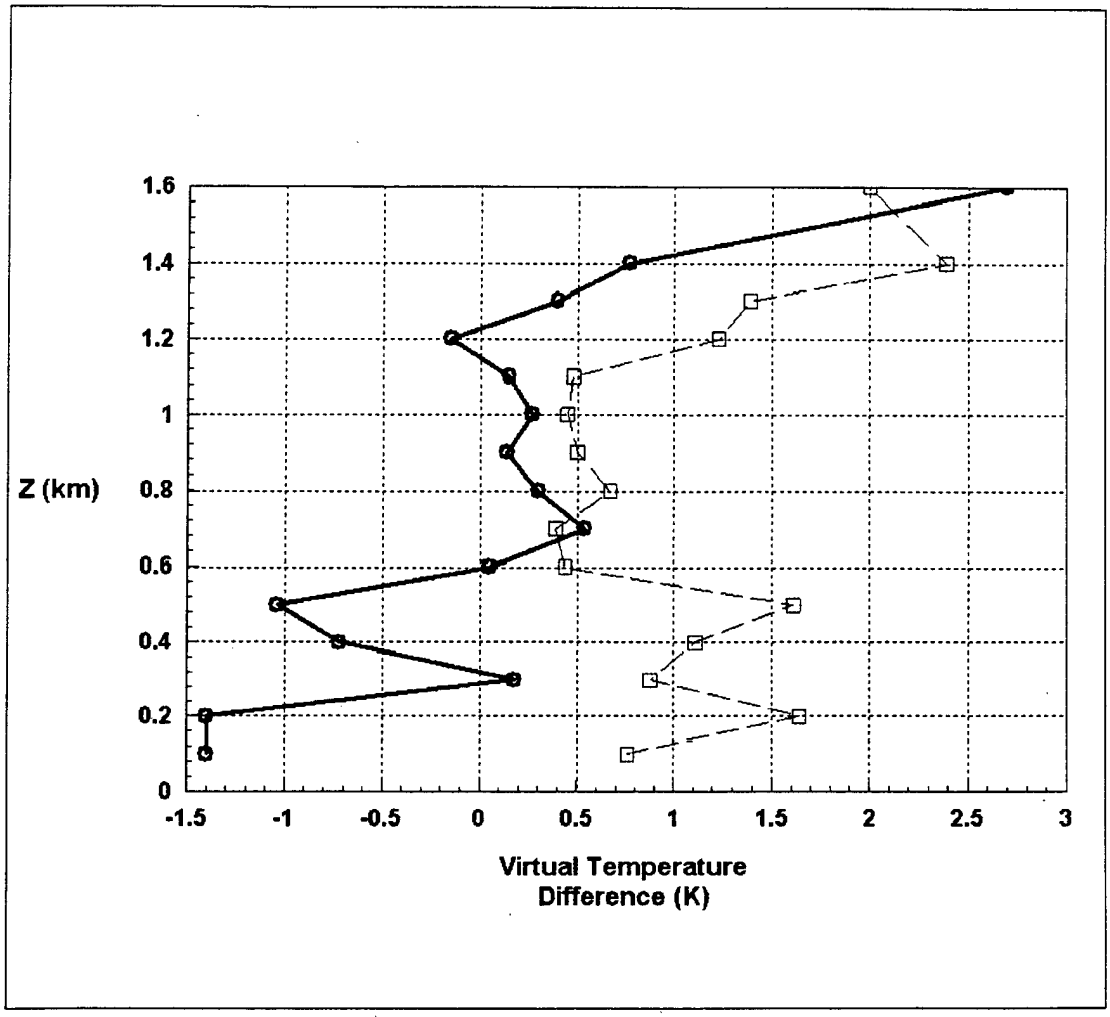

Figure 6. Same as figure 4, but for RASS only.

Figure 3 shows a fairly typical pattern (e.g., accuracy degraded near the tropopause) of standard deviation (σ_T) of T_v differences at satellite levels with values somewhat lower than previously published (Le Marshall; Reale). [7, 8] The merging of satellite and RASS profiles greatly reduced the differences in the lowest few kilometers relative to satellite soundings alone (about 0.5 to 2 °K versus 5 to 8 °K). Figures 3 and 5 show that the magnitude of mean differences and σ_T values for the RASS are fairly small (< 0.5 and < 0.9 °K, respectively, for $0.1 < z < 1.3$ km), except at the highest RASS levels (≥ 1.3 km) and near the surface (≤ 0.1 km).

Figure 4 presents a less common distribution of values with height (z) at satellite levels. The σ_T of T_v differences decreases near the tropopause, and the mean of the differences is high at lower satellite levels in spite of a reduction in magnitude as a result of the merging process. In figures 4 and 6 the RASS values of σ_T are higher at $z \leq 0.5$ km and at $z \geq 1.3$ km. Magnitude of the mean differences for RASS is high at some lower layers, and at 1.6 km. These results are not unexpected. In the lower layers, surface heating and cooling cause greater variability. The higher layers, near the maximum range for RASS, often coincided with the height of the marine inversion. Variability in height and strength of this inversion, and its relationship to location and thickness of combined sounding layers, are significant factors when comparing with rawinsonde soundings.

The lower σ_T near the tropopause during the second period may have arisen as a result of a weaker lapse rate, or little change in it, and possibly also as a result of a lower horizontal temperature gradient near the tropopause over the area in and around the Los Angeles basin during most or all of the second period. The former would tend to reduce inaccuracies in the satellite data due to the inherent smoothing of vertical temperature gradients and errors induced by incorrect height attributed to a satellite value. The latter would tend to lower temperature differences between satellite and rawinsonde that occur because of horizontal distance between satellite sounder field of view and rawinsondJe location. An investigation of sounding data from three stations near the Los Angeles basin indicated that the magnitude of the lapse rate from about 11 to 14 km (below the tropopause) was about 1.2 °Kkm^{-1} to about 1.7 °Kkm^{-1} smaller during the comparison days of the second period (average) depending on the station. Also, the tropopause was about 2 to 3 °K warmer during the second period.

Upper-air maps for 200 hPa (12.1 km < z < 12.5 km), near the top of the combined soundings from the LAFRE, showed a more zonal distribution of tem-

perature during the second period than during the first. The mean and standard deviation of the magnitude of the horizontal lapse rate within 300 km of the test site showed almost no change for the east-west gradient. Small increases in magnitude of mean and standard deviation of about 0.1 to 0.2 °K/100 km each appeared for the north-south gradient from the first to second period. An increase in the north-south gradient would be expected as the distribution of temperature became more zonal. However, the smoothing of horizontal temperature gradients in satellite data (Jedlovec) would tend to further reduce the effect, if noticeable, of those small changes. [6] While the effect on temperature differences between satellite and rawinsonde would have been minimal from the changes in the horizontal gradient noted above (very small increase in σ_T), the more significant decrease in vertical temperature gradient and the warmer tropopause during the second period (relatively large decrease in σ_T) may at least partly explain the reduction in σ_T in the few kilometers below the tropopause.

Table 3 shows means and standard deviations of wind speed differences in meters per second for the radar profiler and satellite (adjusted at the lowest three satellite data levels) relative to rawinsonde. The maximum number of data comparisons by layer are the same as for the T_v comparisons presented above.

Table 3. Means and standard deviations of wind speed differences (ms^{-1}) for 0.3 km layers (indicated sensor - rawinsonde) obtained during the LAFREE.

	September 7-11, 1993		September 17 and 20-23, 1993	
	Radar profiler	Satellite	Radar profiler	Satellite
Mean	0.75	10.84	1.53	8.61
Std. deviation	1.88	8.60	2.75	2.88
No. of layers	14	6	11	6

At times the rawinsonde data may contain serious errors. Fisher et al. present information on the average errors found in several types of rawinsonde systems. [26] To gain an idea of the quality of the rawinsonde data from the LAFRE, soundings were compared from two similar systems (MARWIN and CLASS) receiving data from one sonde. Differences in T_v from comparisons using a single sonde averaged approximately ± 0.2 to 0.4 °K, with maximum differences

of about ± 1 °K. Figure 7 compares wind speed differences between the two systems. The periodic pattern is consistent with other data examined to date. The large differences near and above 3 km are on the high side, but values around ± 1 ms^{-1} are not uncommon. Cogan and Izaguirre presented data showing a few wind direction variations of > 90° in one case during the LAFRE, although wind direction differences for most heights in data examined to date were < 10°. [16] This type of comparison suggests that differences in profiler wind speed and direction of around ± 1 ms^{-1} and 10°, respectively, relative to rawinsonde may be close to the "best" one could expect. A possible partial explanation for the wind speed differences is that the MARWIN software has more extensive built-in checks and smooths the data somewhat. Nevertheless, caution must be taken when using a rawinsonde sounding as a standard, especially in light winds. The user should make sure each sounding contains valid data, and apply appropriate quality controls.

4.2 Wallops Island

Field tests at the NASA Wallops Flight Facility (WFF) on Wallops Island, VA, provided the opportunity to compare MPS wind profiles for the lowest 1.9 km with wind profiles obtained from radar-tracked pibal balloons. An unusual aspect of this experiment as compared with other comparison studies such as the LAFRE and earlier work (e.g., Weber and Wuertz) was the ability to examine the background wind variability at the same time as the comparisons. [24] During the week of July 17 through 21, 1995, for morning and afternoon periods lasting about 1 to 1½ h, two pibals were launched about 3 min apart every 15 min (four to five "pairs" each period). The MPS operated continuously during these periods producing wind profiles every 3 min. For each pibal pair, comparisons were made between the 3 min MPS profile just prior to the second pibal and the second pibal, and between the first and second pibal. Surface values shown were taken from the WFF and MPS surface sensors. The site of the experiment was about 0.2 km west of the ocean, with the MPS located < 50 m east from the pibal launch site. Figures 8 through 11 show the means and standard deviations of the wind speed and direction differences between MPS and second pibal, and pibal pairs for 100 m layers, during July 20, 1995 (nine pairs), and July 21,1995 (five pairs).

The MPS versus pibal comparison for July 18 (not shown) showed significantly greater differences in wind direction than for the other two comparison days (July 20 and 21). The pibal versus pibal comparison for that day also showed somewhat larger differences in wind direction relative to those for the other days.

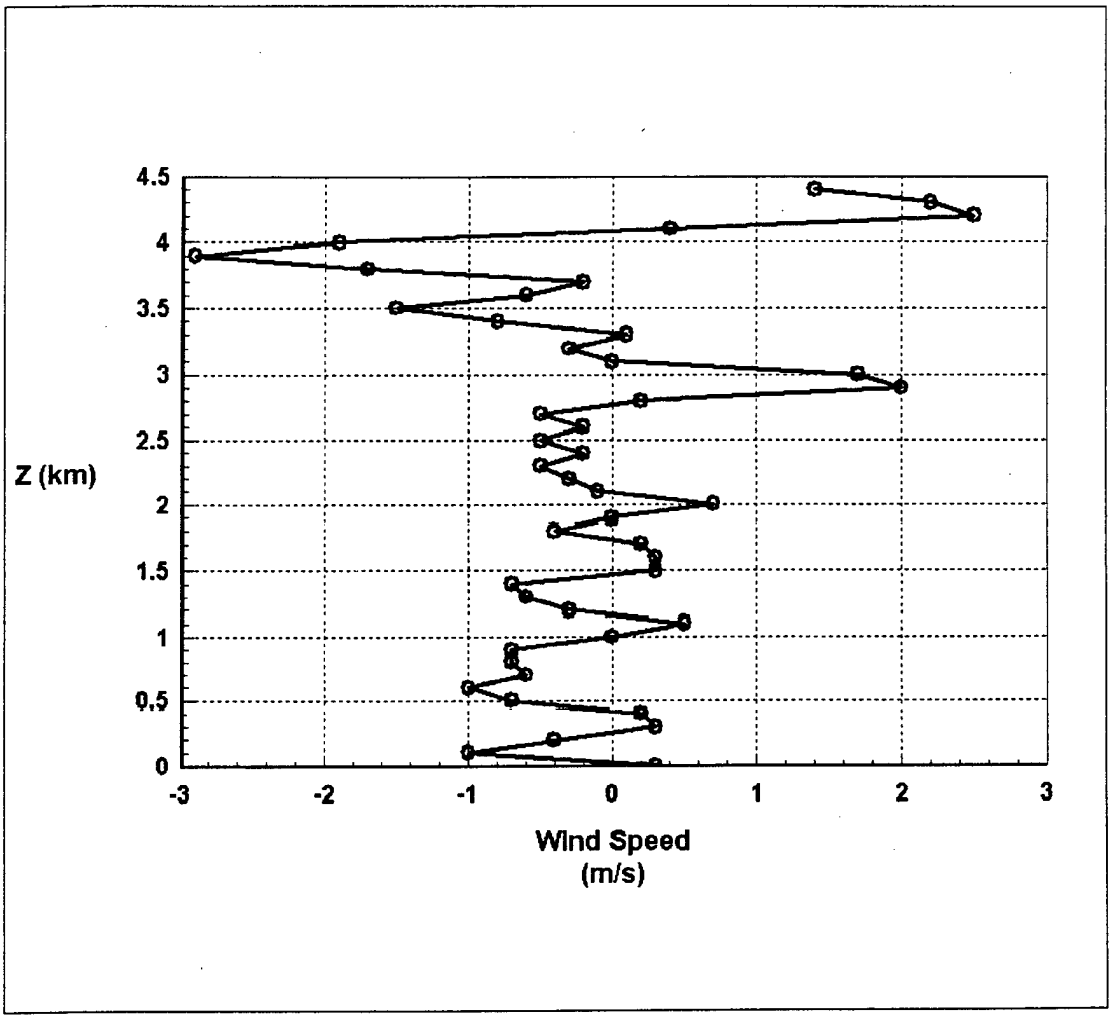

Figure 7. Mean wind speed differences (ms^{-1}) between CLASS and MARWIN systems from LAFRE data. Data gathered by one sonde. Heights are AGL.

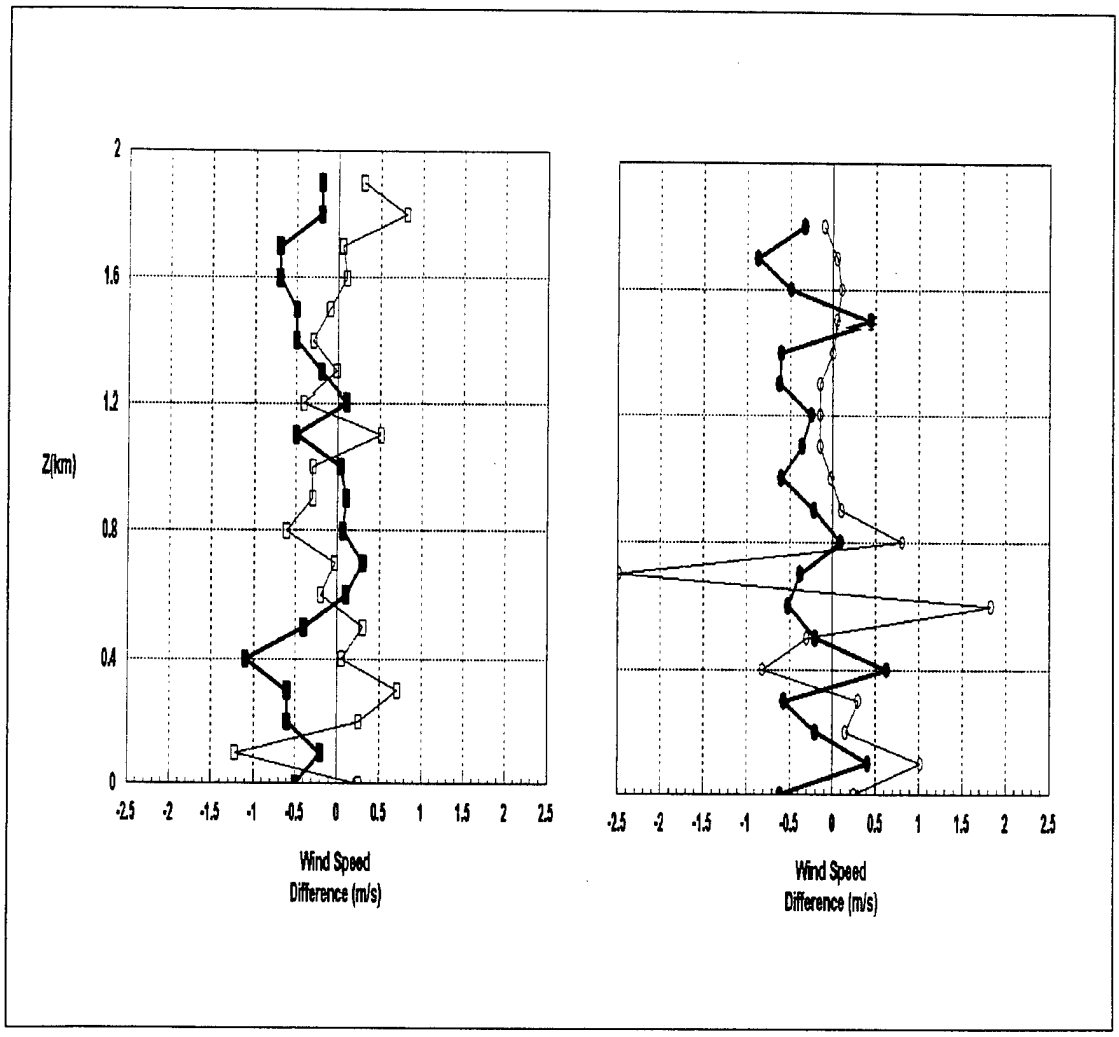

Figure 8. Mean wind speed differences (ms^{-1}) from WFF data. Heights are AGL. Bold curves represent MPS versus pibal, lighter ones represent pibal versus pibal. Left graph (square data points) and right graph (circles) are plots for July 20 and 21, respectively.

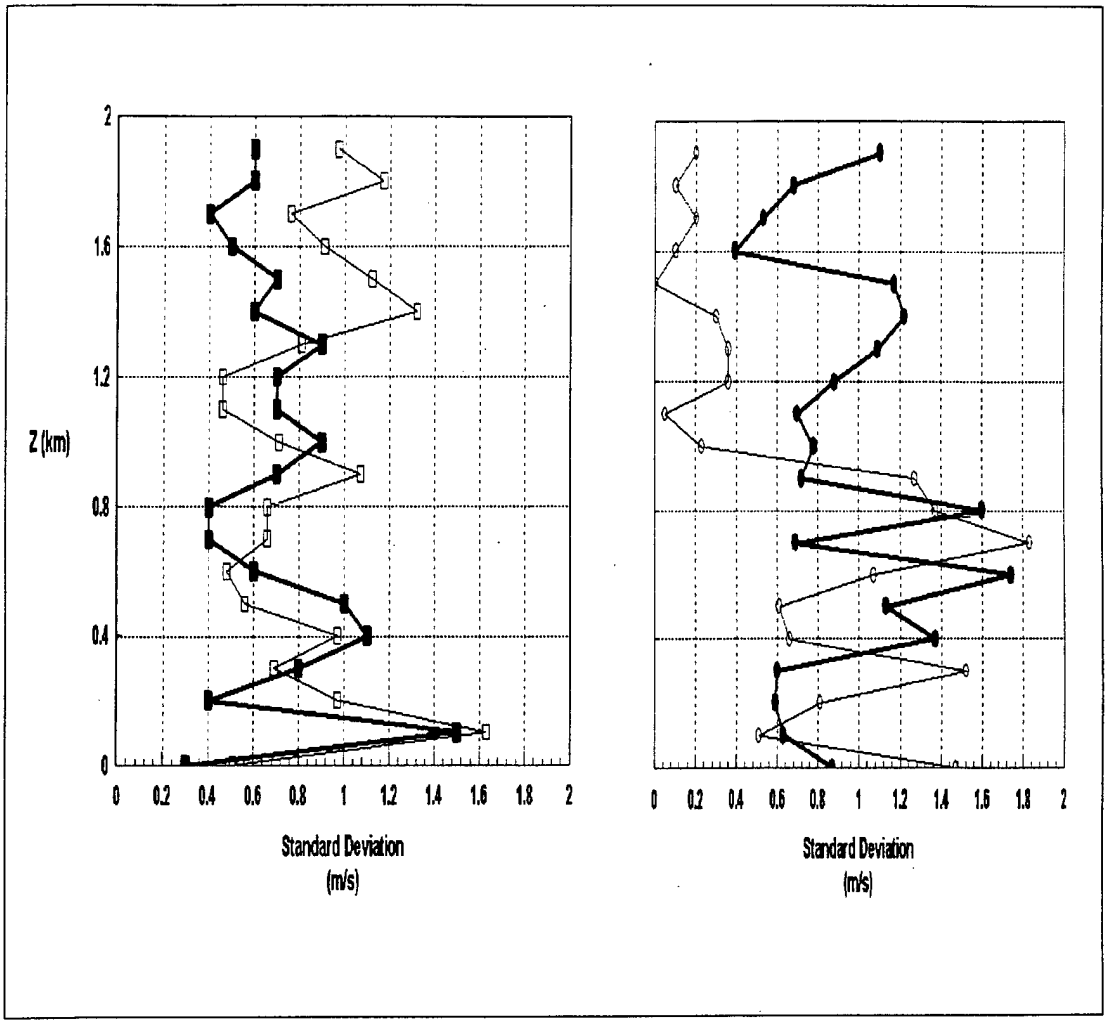

Figure 9. Same as figure 8, except plotted for standard deviation of wind speed differences (ms^{-1}).

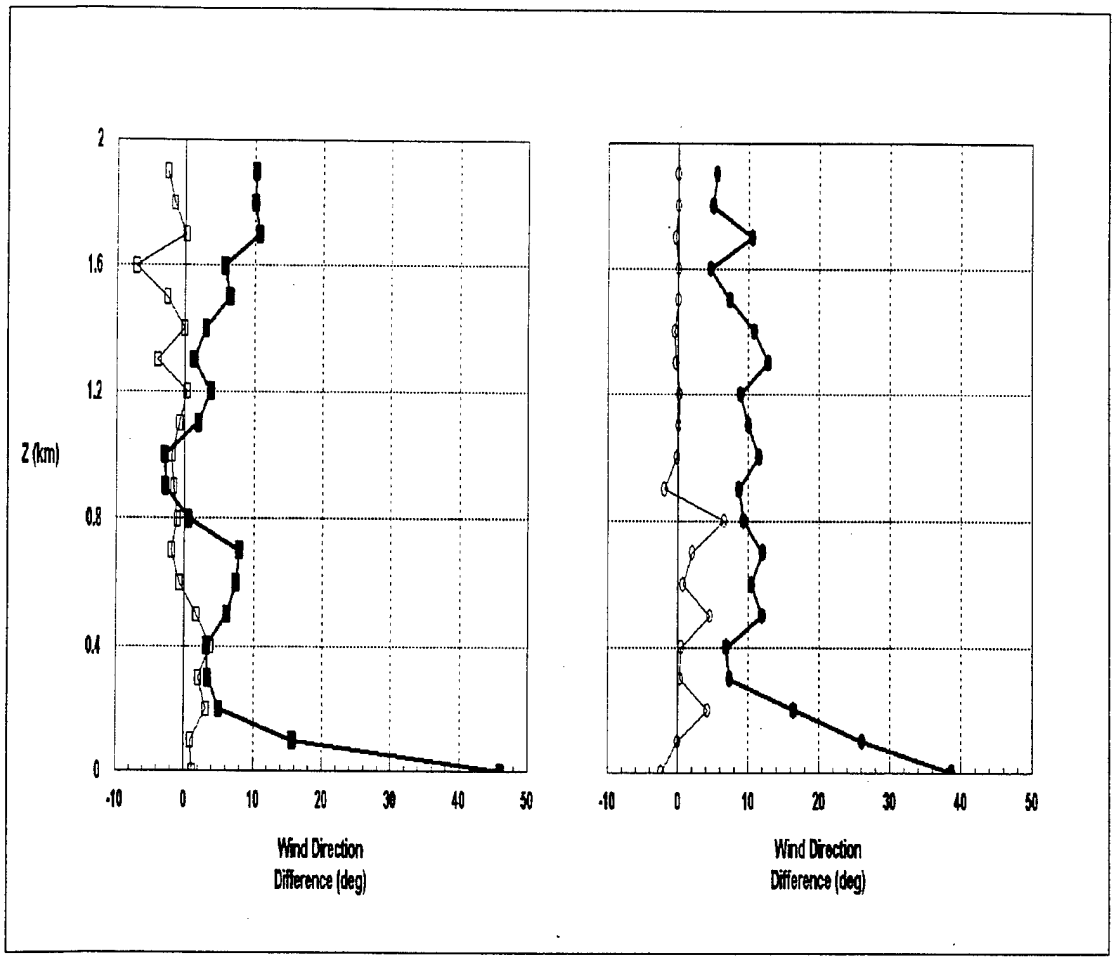

Figure 10. Same as figure 8, except plotted for mean wind direction differences (°).

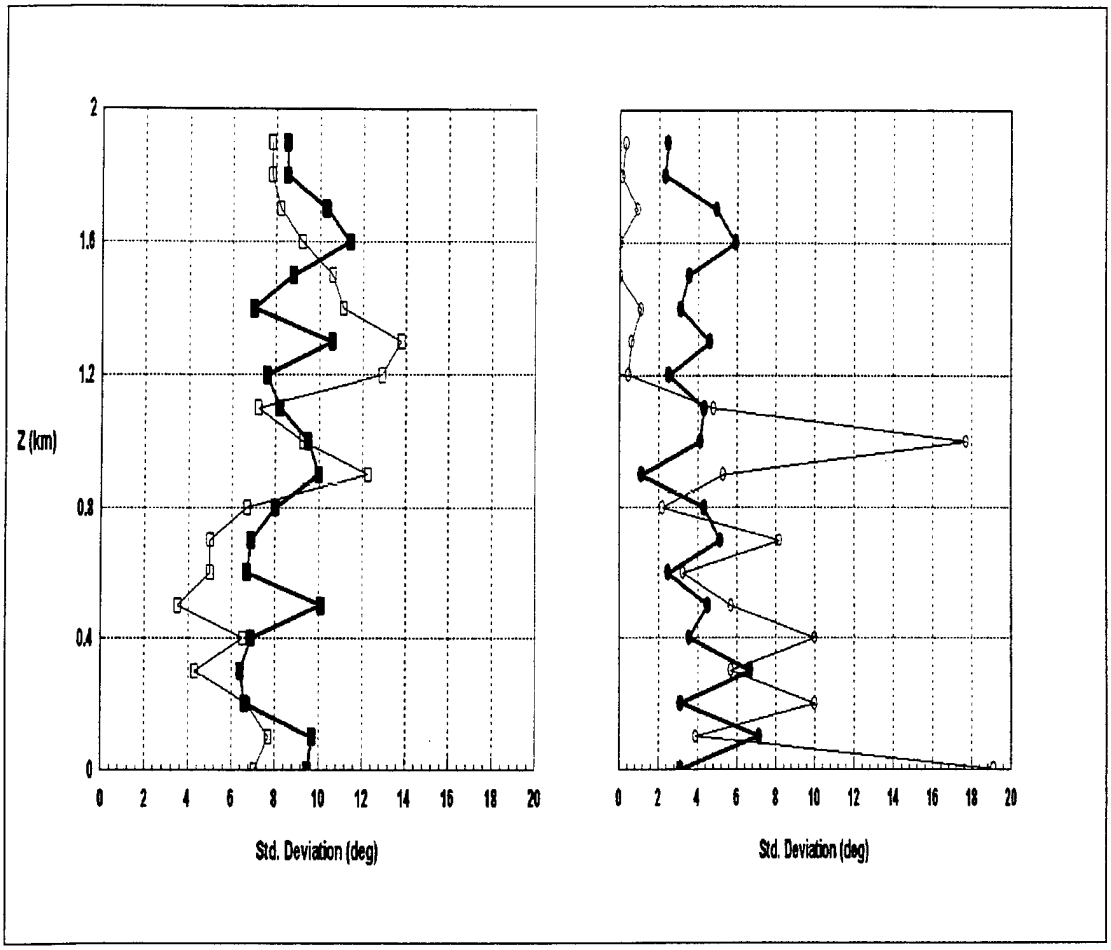

Figure 11. Same as figure 8, except plotted for standard deviation of wind direction differences (°).

The standard deviation of wind direction differences exceeded 10° for pibal versus pibal for heights *(z)* ≤ 0.3 km and z = 1.1 km, and for the MPS versus pibal at $z \leq 0.8$ km and $z = 1.2$ km. The magnitude of mean differences in wind direction between MPS and pibal was ≥ 20° at z = 0.6 km, $0.8 \leq z \leq 1.2$ km, and $1.5 \leq z \leq 1.8$ km (maximum of about 25° at 1.6 km). Magnitude of mean and standard deviation of wind speed differences was somewhat larger at $z \leq$ 0.6 km for the MPS versus pibal. Also, on this day the pibals traveled eastward, passing over the ocean within 1 min after launch. These larger differences were, therefore, not unexpected since the pibals drifted over the ocean after reaching 200 or 300 m in altitude, leaving the highly convective conditions that existed over the land. Later in the afternoon small but intense thunderstorms passed through from the west, forcing the test to be canceled before 1500 EDT (1900 UTC) due to the danger of lightning strikes.

The largest direction difference between the MPS and pibal was at the "surface" (about 5 m AGL) for the latter two days and at 0.1 km on July 18. Both systems relied on surface stations separated by about 10 m horizontally and 1 to 2 m vertically (the WFF anemometer was higher). The location, only about 200 m from the ocean, and the mix of land and water surfaces near the launch site may account for much of the observed direction differences in the lowest 0.1 to 0.2 km. The balloons drifted off roughly to the northwest except on July 18 when, soon after turning toward the east to northeast, they passed over the northern half of the island and then out over the water. Since the ascent rate of the pibals was about 5 ms^{-1} and the average wind speed for most of the test periods was about 5 to 7 ms^{-1} during much of each ascent, the balloon ended up about 2 to 3 km from the MPS and pibal launch site by the time it reached an altitude of 2 km. On July 21 the wind speed at most heights exceeded 10 ms^{-1}, causing the pibal to drift about 4 km by the time it rose to 2 km.

The comparison of wind profiling radar with radar-tracked pibals yielded results for wind speed that appear better than those shown in table 3. The average magnitude of mean differences (0.1 km layers) from the WFF data (figure 8) appears similar to that from the LAFRE data for September 7 through 11, 1993. However, the average of the means from the LAFRE for September 17 and 20 through 23 is considerably larger. The standard deviations of the differences for all layers in figure 9 are less than the average standard deviation of either period in table 3. The average standard deviation between MPS and pibal in figure 9 is about 0.8 ms^{-1}.

The accuracies suggested using data from the WFF experiment (figures 8 through 11) appear better overall than those presented in table 2 for radar profilers, except for wind direction on July 18. The differences between values in figures 8 through 11 and tables 2 and 3, and variations between profiles from pibals launched 3 min apart (also figures 8 through 11), support the idea that at least part of the differences between radar profiler and rawinsonde wind soundings in earlier LAFRE data indeed may be a result of real atmospheric temporal and spatial variation. The data for 18 July, with even larger standard deviations of wind direction differences for both pibal versus pibal and MPS versus pibal than those for 20 and 21 July, suggests that these variations can be significant even over a 3 min time span.

The Wallops Island experiment provided an opportunity to test a new type of surface-based radiometer, developed for ARL by the OPHIR Corporation. This new radiometer, called the Next Generation Radiometer (NGR), incorporates several design advances over the older system (the Passive Microwave Temperature Profiler, or PMTP), including a much smaller size and lighter weight, and, notably, frequency tunability and very precise software control of radiometer frequency in the oxygen bands. The antenna system for the NGR is based on an optical lens that focuses into a corrugated horn antenna.

The PMTP uses Gunn diodes for local oscillators for all measurements. There are four such oscillators limiting measurement to four frequencies. The oscillators also suffer from a tendency to drift in frequency when their temperatures are not precisely controlled, and require frequent calibration to check for drift due to mechanical effects. In the NGR, the oxygen-band local oscillator is a highly stable tunable synthesizer. This frequency tunability of NGR makes it practical to use a larger number of frequencies (for this experiment, 11 frequencies) in the 50-60 GHz sensing band.

In the Wallops experiment, the performance of the radiometers, as measured by comparison with simultaneous radiosonde observations, was comparable at lower levels, but the NGR appeared definitely superior at the higher levels. Figure 12 shows root mean square (RMS) differences for nine comparisons between simultaneous radiosonde observations and corresponding measurements with the current ARL oxygen radiometer system (PMTP) and the OPHIR radiometer (NGR).

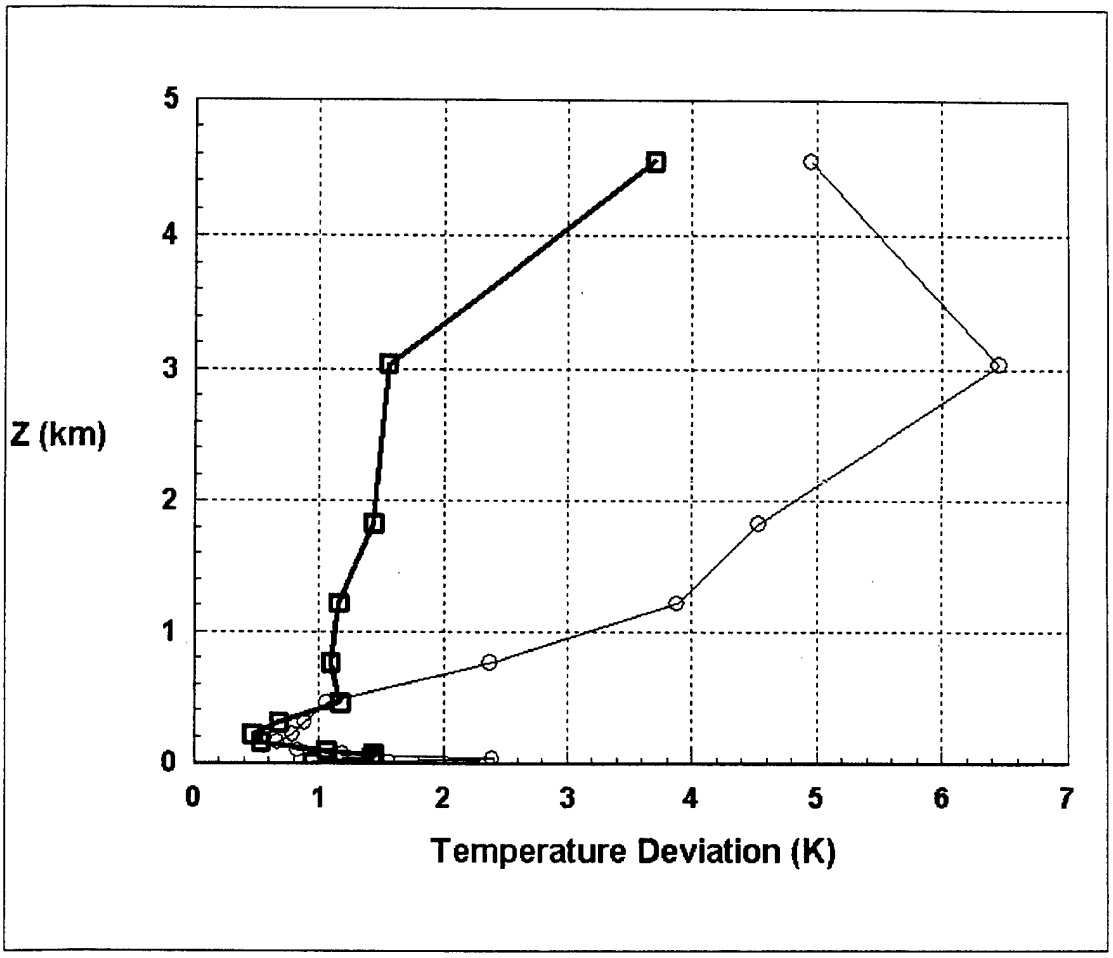

Figure 12. RMS deviations of NGR (bold squares) and PMPT (lighter circles) from concurrent rawindsonde observations.

5. Conclusions

The MPS shows promise as a means of collecting data from a variety of profiling instruments and merging these data into combined meteorological soundings for near real-time operational applications. The merging method provides soundings with an accuracy in temperature (or virtual temperature) comparable to rawinsonde soundings or to other currently published methods of combining ground-based and satellite data. While the microwave radiometer component of the MPS uses *a priori* information, the merging algorithm has the advantage of not being site specific, and *a priori* data sets are not required as in statistical merging techniques. It also may be used to combine profiles of other meteorological variables. However, the accuracy of wind velocity values above the maximum radar data level is limited by the errors in current methods of deriving wind velocity from satellite sounder data. New ways to derive satellite wind velocities are being investigated. In the interim, merging wind data from conventional systems (e.g., rawinsondes) for the upper part of the sounding may be the only viable alternative.

The combining algorithm is not limited to the MPS. It also can be applied to other suites of instruments capable of measuring profiles. Existing facilities where this algorithm may prove useful include the NOAA NPN, and systems at sites within or near airports and at government test ranges. The basic method may be applied to airborne systems as well.

The data provided by the MPS will have a variety of civilian and military applications. The MPS can provide timely support for airfield operations, giving, for example, near real-time indications of potentially hazardous wind conditions. As the Los Angeles Free Radical Experiment showed, this type of system can be invaluable for pollution studies. The ability to generate a picture of very short-term flow and virtual temperature patterns in the lower troposphere can lead to a better understanding of the atmosphere and to better modeling at smaller scales.

References

1. Barth, M. F., R. B. Chadwick, and D. W. van de Kamp, "Data Processing Algorithms Used by NOAA's Wind Profiler Demonstration Network," *Ann. Geophysicae,* **12,** pp. 518-528, 1994.

2. Ralph, R. M., P. J. Neiman, D. W. van de Kamp, and D. C. Law, "Using Spectral Moment Data from NOAA's 404-MHz Radar Wind Profilers to Observe Precipitation," *Bull. Amer. Metero. Soc.,* **76,** pp. 1717-1739, 1995.

3. Weber, B. L., D. B. Wuertz, R. G. Strauch, D. A. Merritt, K. P. Moran, D. C. Law, D. Van de Kamp, R. B. Chadwick, M. H. Ackley, M. F. Barth, N. L. Abshire, P. A. Miller, and T. W. Schlatter, "Preliminary Evaluation of the First NOAA Demonstration Network Wind Profiler," *J. Atmos. Ocean. Technol.,* **7,** pp. 909-918, 1990.

4. Strauch, R. G., D. A. Merritt, K. P. Moran, K. B. Earnshaw, and D. C. Welsh, "The Colorado Wind Profiling Network," *J. Atmos. Ocean. Technol.,* **1,** pp. 37-49, 1984.

5. Orlanski, I., "A Rational Subdivision of Scales for Atmospheric Processes," *Bull. Amer. Meteor. Soc.,* **5,** pp. 527-530, 1975.

6. Jedlovec, G. J., "An Evaluation and Comparison of Vertical Profile Data from the VISSR Atmospheric Sounder (VAS)," *J. Atmos. Ocean. Technol.,* **2,** 559-581, 1985.

7. Le Marshall, J. F., "An Intercomparison of Temperature and Moisture Fields Derived from TIROS Operational Vertical Sounder Data by Different Retrieval Techniques, Part I: Basic Statistics," *J. Appl. Meteor.,* **27,** pp. 1282-1293, 1988.

8. Reale, A. L., *Baseline Upper Air Network (BAUN) Final Report,* NOAA Technical Report NESDIS 52, U.S. Dept. of Commerce, NOAA/NESDIS, Washington, DC, 57 pp., 1990.

9. Franklin, J. L. and S. J. Lord, "Comparisons of VAS and Omega Dropwindsonde Thermodynamic Data in the Environment of Hurricane Debby (1982)," *Mon. Wea. Rev.,* **116,** pp. 1690-1701, 1988.

10. Heacock, L. E., Ed., *Envirosat-2000 Report: Comparison of the Defense Meteorological Satellite Program (DMSP) and the NOAA Polar-Orbiting Operational Environmental Satellite (POES) Program,* DTIC acquisition number ADA165118, National Oceanic and Atmospheric Administration, National Environmental Satellite, Data, and Information Service, 426 pp., 1985.

11. Shenk, W. E., T. H. Vonder Haar, and W. L. Smith, "An Evaluation of Observations from Satellites for the Study and Prediction of Mesoscale Events and Cyclone Events," *Bull. Amer. Meteor. Soc.,* **68,** pp. 21-35, 1987.

12. Swadley, S. D., and J. Chandler, "The Defense Meteorological Satellite Program's Special Sensor Microwave Imager/Sounder (SSMIS): Hardware and Retrieval Algorithms. Preprints," Sixth Conference on Satellite Meteorology and Oceanography, Atlanta, GA, Amer. Meteor. Soc., pp. 457-461, 1992.

13. Wolfe, D., B. Weber, D. Weurtz, D. Welsh, D. Merritt, S. King, R. Fritz, K. Moran, M. Simon, A. Simon, J. Cogan, D. Littell, and E. Measure, "An Overview of the Mobile Profiler System (MPS): Preliminary Results from Field Tests During the Los Angeles Free Radical Study," *Bull. Amer. Meteor. Soc., 76,* pp. 523-534, 1995.

14. Parsons, D., W. Dabberdt, H. Cole, T. Hock, C. Martin, A. Barrett, E. Miller, M. Spowart, M. Howard, W. Ecklund, D. Carter, K. Gage, and J. Wilson, "The Integrated Sounding System: Description and Preliminary Observations from TOGA COARE" *Bull. Amer. Meteor. Soc.,* **75,** pp. 553-567, 1994.

15. Stokes, G. M. and S. E. Schwartz, "The Atmospheric Radiation Measurement (ARM) Program: Programmatic Background and Design of the Cloud and Radiation Testbed," *Bull. Amer. Meteor. Soc.,* **75,** pp. 1201-1221, 1994.

16. Cogan, J. and A. Izaguirre, "Test Results from a Mobile Profiler System," *Meteor. Appl.,* **2,** pp. 97-107, 1995.

17. Cogan, J. and A. Izaguirre, *A Preliminary Method for Atmospheric Soundings in Near Real Time Using Satellite and Ground-Based Remotely Sensed Data,* ARL-TR-240, DTIC acquisition number ADA274381, U.S. Army Research Laboratory, White Sands Missile Range, NM, 45 pp., 1993.

18. Westwater, E. R., W. B. Sweezy, L. M. McMillin, and C. Dean, "Determination of Atmospheric Temperature from a Statistical Combination of Ground-Based Profiler and Operational NOAA 6/7 Satellite Retrievals," *J. Climate Appl. Meteor.,* **23,** pp. 689-703, 1984a.

19. Westwater, E. R., W. Zhendui, N. C. Grody, and L. M. McMillin, "Remote Sensing of Temperature Profiles by a Combination of Ground-Based Profiler and Satellite-Based MSU Radiometric Observations, Proceedings," Conf. on Satellite/Remote Sensing and Applications, Clearwater, FL, Amer. Meteor. Soc., pp. 191-196, 1984b.

20. Schroeder, J. A., E. R. Westwater, P. T. May, and L. M. McMillin, "Prospects for Temperature Sounding with Satellite and Ground-Based RASS Measurements," *J. Atmos. and Ocean. Technol.,* **8,** pp. 506-513, 1991.

21. Moran, K. P. and R. G. Strauch, "The Accuracy of RASS Temperature Measurements Corrected for Vertical Air Motion" *J. Atmos. Ocean. Technol.,* **11,** pp. 995-1001, 1994.

22. Flowers, W., L. Parker, G. Hoidale, E. Santonin, and J. Hines, *Evaluation of a 924 MHz Wind Profiling Radar,* ARL-CR-101, DTIC acquisition number ADA283782, U.S. Army Research Laboratory, White Sands Missile Range, NM, 195 pp., 1994.

23. Okrasinski, R. J. and R. O. Olsen, "Intercomparison of Wind Measurements from Two Doppler SODARS, a UHF Profiling Radar, Rawinsondes, and In Situ Tower Sensors. Extended Abstracts," Symposium on Lower Tropospheric Profiling: Needs and Technologies, Boulder, CO, Amer. Meteor. Soc., pp. 121-122, 1991.

24. Weber, B. L., and D. B. Wuertz, "Comparison of Rawinsonde and Wind Profiler Radar Measurements," *J. Atmos. Ocean. Technol.,* **7,** pp. 157-174, 1990.

25. May, P. T., K. P. Moran, and R. G. Strauch, "The Accuracy of RASS Temperature Measurements," *J. Appl. Meteor.,* **28,** pp. 1329-1335, 1989.

26. Fisher, E. E., F. Brousaides, E. Keppel, F. J. Schmidlin, H. C. Herring, and D. Tolzene, *Meteorological Data Error Estimates,* Document 353-87, Meteorology Group, Range Commanders Council, White Sands Missile Range, NM, 23 pp. [Available from U.S. Army Research Laboratory, AMSRL-IS-EA, White Sands Missile Range, NM 88002-5501], 1987.

27. Wilczak, J. M., R.G. Strauch, F. M. Ralph, B. L. Weber, D. A. Merritt, J. R. Jordan, D. E. Wolfe, L. K. Lewis, D. B. Wuertz, J. E. Gaynor, S. A. McLaughlin, R. R. Rogers, A. C. Riddle, and T. S. Dye, "Contamination of Wind Profiler Data by Migrating Birds: Characteristics of Corrupted Data and Potential Solutions," *J. Atmos. Ocean. Technol.,* **12,** pp. 449-467, 1995.

28. Merritt, D., "A Statistical Averaging Method for Wind Profile Doppler Spectra," *J. Atmos. Ocean. Technol.,* **12,** pp. 985-995, 1995.

Acronyms and Abbreviations

AGL	above ground level
ARL	U.S. Army Research Laboratory
BED	Battlefield Environment Division
CLASS	Cross-chain Loran Atmospheric Sounding System
DMSP	Defense Meteorological Satellite Program
ETL	Environmental Technology Laboratory
LAFRE	Los Angeles Free Radical Experiments
MPS	Mobile Profiler System
NGR	Next Generation Radiometer
NOAA	National Oceanic and Atmospheric Administration
NPN	National Profiler Network
PMTP	Passive Microwave Temperature Profiler
R	accuracy ratio
RASS	Radio Acoustic Sounding System
RMS	root mean square
T	temperature
T_v	virtual temperature
WSMR	White Sands Missile Range
WFF	Wallops Flight Facility

Distribution

	Copies
NASA MARSHALL SPACE FLT CTR ATMOSPHERIC SCIENCES DIV E501 ATTN DR FICHTL HUNTSVILLE AL 35802	1
NASA SPACE FLT CTR ATMOSPHERIC SCIENCES DIV CODE ED 41 1 HUNTSVILLE AL 35812	1
US ARMY MISSILE CMND AMSMI RD AC AD ATTN DR PETERSON REDSTONE ARSENAL AL 35898-5242	1
US ARMY MISSILE CMND AMSMI RD AS SS ATTN MR H F ANDERSON REDSTONE ARSENAL AL 35898-5253	1
US ARMY MISSILE CMND AMSMI RD AS SS ATTN MR B WILLIAMS REDSTONE ARSENAL AL 35898-5253	1
US ARMY MISSILE CMND AMSMI RD DE SE ATTN MR GORDON LILL JR REDSTONE ARSENAL AL 35898-5245	1
US ARMY MISSILE CMND REDSTONE SCI INFO CTR AMSMI RD CS R DOC REDSTONE ARSENAL AL 35898-5241	1
US ARMY MISSILE CMND AMSMI REDSTONE ARSENAL AL 35898-5253	1
PACIFIC MISSILE TEST CTR GEOPHYSICS DIV ATTN CODE 3250 POINT MUGU CA 93042-5000	1
NAVAL OCEAN SYST CTR CODE 54 ATTN DR RICHTER SAN DIEGO CA 52152-5000	1
METEOROLOGIST IN CHARGE KWAJALEIN MISSILE RANGE PO BOX 67 APO SAN FRANCISCO CA 96555	1

DEPT OF COMMERCE CTR
MOUNTAIN ADMINISTRATION
SPPRT CTR LIBRARY R 51
325 S BROADWAY
BOULDER CO 80303 — 1

DR HANS J LIEBE
NTIA ITS S 3
325 S BROADWAY
BOULDER CO 80303 — 1

NCAR LIBRARY SERIALS
NATL CTR FOR ATMOS RSCH
PO BOX 3000
BOULDER CO 80307-3000 — 1

DEPT OF COMMERCE CTR
325 S BROADWAY
BOULDER CO 80303 — 1

HEADQUARTERS DEPT OF ARMY
DAMI POI
ATTN LEE PAGE
WASHINGTON DC 20310-1067 — 1

MIL ASST FOR ENV SCI OFC
OF THE UNDERSEC OF DEFNS
FOR RSCH & ENGR R&AT E LS
PENTAGON ROOM 3D129
WASHINGTON DC 20301-3080 — 1

DEAN RMD
ATTN DR GOMEZ
WASHINGTON DC 20314 — 1

US ARMY INFANTRY
ATSH CD CS OR
ATTN DR E DUTOIT
FT BENNING GA 30905-5090 — 1

HQ AFWA/DNX
106 PEACEKEEPER DR STE 2N3
OFFUTT AFB NE 68113-4039 — 1

PHILLIPS LABORATORY
PL LYP
ATTN MR CHISHOLM
HANSCOM AFB MA 01731-5000 — 1

ATMOSPHERIC SCI DIV
GEOPHYISCS DIRCTRT
PHILLIPS LABORATORY
HANSCOM AFB MA 01731-5000 — 1

PHILLIPS LABORATORY
PL LYP 3
HANSCOM AFB MA 01731-5000 — 1

US ARMY MATERIEL SYST
ANALYSIS ACTIVITY
AMXSY
ATTN MR H COHEN
APG MD 21005-5071 1

US ARMY MATERIEL SYST
ANALYSIS ACTIVITY
AMXSY AT
ATTN MR CAMPBELL
APG MD 21005-5071 1

US ARMY MATERIEL SYST
ANALYSIS ACTIVITY
AMXSY CR
ATTN MR MARCHET
APG MD 21005-5071 1

ARL CHEMICAL BIOLOGY
NUC EFFECTS DIV
AMSRL SL CO
APG MD 21010-5423 1

US ARMY MATERIEL SYST
ANALYSIS ACTIVITY
AMSXY
APG MD 21005-5071 1

ARMY RESEARCH LABORATORY
AMSRL D
2800 POWDER MILL ROAD
ADELPHI MD 20783-1145 1

ARMY RESEARCH LABORATORY
AMSRL OP CI SD TL
2800 POWDER MILL ROAD
ADELPHI MD 20783-1145 1

ARMY RESEARCH LABORATORY
AMSRL CI LL
ADELPHI MD 20703-1197 1

ARMY RESEARCH LABORATORY
AMSRL SS SH
ATTN DR SZTANKAY
2800 POWDER MILL ROAD
ADELPHI MD 20783-1145 1

ARMY RESEARCH LABORATORY
AMSRL IS
ATTN J GANTT
2800 POWDER MILL ROAD
ADELPHI MD 20783-1197 1

ARMY RESEARCH LABORATORY
AMSRL
2800 POWDER MILL ROAD
ADELPHI MD 20783-1145 1

NATIONAL SECURITY AGCY W21
ATTN DR LONGBOTHUM
9800 SAVAGE ROAD
FT GEORGE G MEADE MD 20755-6000 1

US ARMY RSRC OFC
ATTN AMXRO GS DR BACH
PO BOX 12211
RTP NC 27009 1

DR JERRY DAVIS
NCSU
PO BOX 8208
RALEIGH NC 27650-8208 1

US ARMY CECRL
CECRL GP
ATTN DR DETSCH
HANOVER NH 03755-1290 1

US ARMY ARDEC
SMCAR IMI I BLDG 59
DOVER NJ 07806-5000 1

ARMY DUGWAY PROVING GRD
STEDP MT DA L 3
DUGWAY UT 84022-5000 1

ARMY DUGWAY PROVING GRD
STEDP MT M
ATTN MR BOWERS
DUGWAY UT 84022-5000 1

DEPT OF THE AIR FORCE
OL A 2D WEATHER SQUAD MAC
HOLLOMAN AFB NM 88330-5000 1

PL WE
KIRTLAND AFB NM 87118-6008 1

USAF ROME LAB TECH
CORRIDOR W STE 262 RL SUL
26 ELECTR PKWY BLD 106
GRIFFISS AFB NY 13441-4514 1

AFMC DOW
WRIGHT PATTERSON AFB OH 45433-5000 1

US ARMY FIELD ARTILLERY SCHOOL
ATSF TSM TA
FT SILL OK 73503-5600 1

US ARMY FOREIGN SCI TECH CTR
CM
220 7TH STREET NE
CHARLOTTESVILLE VA 22448-5000 1

NAVAL SURFACE WEAPONS CTR
CODE G63
DAHLGREN VA 22448-5000 1

US ARMY OEC
CSTE EFS
PARK CENTER IV
4501 FORD AVE
ALEXANDRIA VA 22302-1458 1

US ARMY CORPS OF ENGRS
ENGR TOPOGRAPHICS LAB
ETL GS LB
FT BELVOIR VA 22060 1

US ARMY TOPO ENGR CTR
CETEC ZC 1
FT BELVOIR VA 22060-5546 1

SCI AND TECHNOLOGY
101 RESEARCH DRIVE
HAMPTON VA 23666-1340 1

US ARMY NUCLEAR CML AGCY
MONA ZB BLDG 2073
SPRINGFIELD VA 22150-3198 1

USATRADOC
ATCD FA
FT MONROE VA 23651-5170 1

ATRC WSS R
WSMR NM 88002-5502 1

ARMY RESEARCH LABORATORY
AMSRL IS S
INFO SCI & TECH DIR
WSMR NM 88002-5501 1

ARMY RESEARCH LABORATORY
AMSRL IS E
INFO SCI & TECH DIR
WSMR NM 88002-5501 1

ARMY RESEARCH LABORATORY
AMSRL IS W
INFO SCI & TECH DIR
WSMR NM 88002-5501 1

DTIC
8725 JOHN J KINGMAN RD
STE 0944
FT BELVOIR VA 22060-6218 1

US ARMY MISSILE CMND
AMSMI
REDSTONE ARSENAL AL 35898-5243 1

US ARMY DUGWAY PROVING GRD STEDP3 DUGWAY UT 84022-5000	1
USTRADOC ATCD FA FT MONROE VA 23651-5170	1
WSMR TECH LIBRARY BR STEWS IM IT WSMR NM 88002	1
ARMY RESEARCH LABORATORY AMSRL IS EA BATTLEFIELD ENVIR DIV ATTN D BROWN WSMR NM 88002-5501	1
ARMY RESEARCH LABORATORY AMSRL IS EA BATTLEFIELD ENVIR DIV ATTN E MEASURE WSMR NM 88002-5501	10
ARMY RESEARCH LABORATORY AMSRL IS EA BATTLEFIELD ENVIR DIV ATTN J COGAN WSMR NM 88002-5501	20
Record copy	1
TOTAL	95